Image Processing, Electronics and Computers
L. Trajkovic et al. (Eds.)

doi:10.3233/ATDE240475

Virtual Roots: Multiple View Dataset Designed by Unity 3D

Peiliang QIN[a,b], Rongjing HONG[a,1] and Saru KUMARI[c]
[a] *School of Mechanical and Power Engineering, Nanjing Tech University, Nanjing, China*
[b] *Division of Science and Technology Industry, Suzhou Polytechnic Institute of Agriculture, Suzhou, China*
[c] *Department of Mathematics, Ch. Charan Singh University, Meerut, India*

Abstract. 3D reconstruction and visualization of plants are of great research value for their physiological characteristics. Large-scale datasets are required to train 3D reconstruction algorithms. Most of the current 3D plant datasets only focus on the parts above the ground surface. Roots, as the half below ground, are also critical for plant growth. There are few efforts to generate 3D root datasets. Existing 3D plant root datasets only contain a very limited number of reconstructed 3D models and the lack of ground truth, mainly because of the complexity of root structures and the inconvenience of obtaining root images and ground truth 3D structures. This paper creates a large virtual 3D plant root benchmark dataset, which not only contains extensive 3D root models; but also has 2D images captured from various angles, involving 1.2K 3D root structures and over 80K 2D root images. This large plant dataset enables testing of multiple 3D reconstruction algorithms to verify the reliability of the algorithms. Finally, multiple commonly used 3D reconstruction algorithms and the most recent state-of-the-art 3D modeling methods are tested on this dataset, which demonstrates the superb research values of this dataset to advance the 3D root modeling research.

Keywords. Image processing, multiple view geometry, three-dimensional reconstruction, benchmark dataset

1. Introduction

Image processing is a technology that uses computer to analyze images, and three-dimensional reconstruction is an important research direction in the field of image processing. Roots, which have capable of absorbing water and nutrients from the soil, are vital organs of plants. Therefore, the growth state of roots has a crucial role in the growth state of plants [1]. By analyzing the 3D root structures, agriculture professionals can know the growth status of plants and take proper action. However, plant roots are buried in the soil, which makes them difficult to observe directly. The degree of root differentiation is high, and their architectures are complex, which makes it difficult to quantify.

There is existing research regarding 3D plant reconstruction. Wang et al. used 3D reconstruction technology on plant canopy structure measurement [2]. Yandun et al.

[1] Corresponding Author: Rongjing HONG, hrj@njtech.edu.cn.

employed Visual 3D Reconstruction of Fruit Trees for Robotic Manipulation [3]. Zhu et al. applied a low-cost 3D reconstruction technique to obtain phenotypic developmental changes in soybean plants [4].

However, there is little research on the 3D reconstruction technologies of plant roots that differ dramatically from other objects. The 3D root shapes can help analyze the root morphological information; and predict the health and growth state of the plant, which is of great significance for the study of plant growth status. Therefore, the 3D reconstruction of plant roots is beneficial to the development of agriculture; but also reduces the complexity of management; and has broad application prospects in agriculture.

Compared with plants above the ground, roots are difficult to observe because they are buried under the ground and maintain extremely complicated shapes. One of the traditional sampling methods is the Minirhizotron system (MRS) [5]; this is a way of using transparent tubes installed in the soil to record the growth of the roots. Another sampling method is ground penetrating radar, but the accuracy of ground penetrating radar is not high enough, and the obtained 3D model of the root is different from the real root, so it cannot reflect the real condition of the root.

The model-based 3D reconstruction method has attracted more and more attention from researchers; because this method has the advantages of high precision and good real-time performance; so it has been used in life and scientific research work, such as bone restoration, cultural relics protection, aerospace, and navigation, etc. In these existing root datasets, images are composed of various states, including different root morphology, root age, and root depth, but there is no uniform standard. Besides, the labels of existing datasets about roots are also unclear. These issues make it difficult for existing root datasets to be widely used.

In this work, we made a dataset containing two kinds of plant roots, namely the root of apple seedlings and the root of sweet potato. Apple has thick and scattered roots with complex shapes, and the root of sweet potato are relatively thin and scattered. Our dataset contains 800 models of apple seedling roots and 400 models of sweet potato roots. In addition, we rotated the 3D model of each root by an angle every 10 degrees in the X and Y axes, then sampled its 2D image. Therefore each model in our dataset also contains 72 images from different angles. Furthermore, our dataset has ground truth compared to the other root datasets, which can facilitate researchers to test their 3D reconstruction algorithms.

2. Related Work

2.1. Image Datasets

There are various datasets in the field of plants, most of these are in the form of images, but datasets about roots are rarer. For example, the Root Cowpea Diversity panel [6], the Plant Seedlings Dataset [7], and the FruitVeg-81 Dataset [8].

These mentioned above, only the Root Cowpea Diversity panel is the dataset about plant roots, but it has no ground truth. The Plant Seedlings Dataset has a good physical resolution, so the overall growth characteristics of the plants can be extracted, which to some extent, can observe the plant's health. The other datasets are about the leaves or fruits of plants; they can only reflect the condition of a certain part of plants and usually have no ground truth too. The ideal 3D reconstruction results need to obtain the

3D features of the object; these 3D features have various forms, such as depth maps, point clouds, or grids. Good features should have good discrimination, robustness, invariance, and computational efficiency. Therefore, for 3D reconstruction tasks, a well-developed 3D dataset is particularly important.

2.2. 3D Model Datasets

In recent years, with the development of 3D reconstruction technology, there are more and more corresponding 3D datasets. Stereo matching datasets mainly include the KITTI Dataset [9], the Scene Flow Dataset [10], and the HCI Robust Vision Challenge Dataset [11], to name a few. KITTI is currently one of the most important test sets in the field of autonomous driving; it contains scenes that many street environments may encounter. Scene Flow is a large-scale synthetic dataset for training deep stereo-matching networks; it is the dense or semi-dense 3D motion field of a scene that moves completely or partially with respect to a camera. HCI Robust Vision Challenge Dataset is a dataset for a stereo or optical flow algorithm challenge; it has multiple real-world scenes that contain instances of challenging phenomena occur in everyday traffic scenarios.

2.3. 3D Reconstruction Algorithms

3D reconstruction is a hot topic in the field of computer graphics and computer vision. One of the very popular 3D reconstruction methods is to use images as input to reconstruct 3D models in the scene. These 3D reconstruction algorithms can be divided into two categories: (1) 3D reconstruction algorithms based on traditional multi-view geometry; (2) 3D reconstruction algorithms based on deep learning.

Traditional 3D reconstruction algorithms can be divided into active and passive according to whether the sensor has a light source. Active type means that the sensor actively irradiates the object with a signal; and then relies on the analysis of the returned signal to obtain three-dimensional information about the object. Such as structured light [12] and laser triangulation [13]. Different from the active type, the passive type directly obtains the RGB image through the ambient light source and then analyzes the acquired RGB image according to the multi-view geometric principle, thereby extracting the three-dimensional information of the object, like monocular vision [14], polyocular vision [15], etc.

In recent years, with the development of deep learning, there has been more and more research on 3D reconstruction relying on deep learning. 3D reconstruction algorithms based on deep learning are mainly divided into two categories: (1) Fusion of deep learning; and traditional 3D reconstruction algorithms, like Deep VO [16]; (2) 3D reconstruction directly through deep learning algorithms, such as 3D-R2N2 [17], 3D Point Clouds [18].

3. Dataset Generation

In this section, we will introduce the generation process of our dataset, describe details of 3D models in our dataset, and how we extracted images from these 3D models. The 3D models in our dataset are all designed by Unity3D, which is a real-time 3D content

creation platform that can allow users to easily create 3D works. Through Unity 3D, we can set the details of every root in our dataset, such as diameter, number of branches, etc.

3.1. Apple Seedling Root 3D Model Design

The apple tree is one of the common rose plants that is distributed all over the world and can represent general fruit tree types. Therefore, we chose the root of the apple seedling as the prototype of the 3D models. By observing the root structure of the real apple seedling, we found that it contains a stem and several branches, and the diameter of the stem is the largest. Usually, the stem is also the longest of all rhizomes. Compared with the stem, the diameter of the branches is slightly smaller, and the growth directions of the stem and branches are very complicated; some even appear entangled and knotted.

In the design interface of Unity3D, we determined the shape of the stem through random numbers, and by setting different values for each root randomly, the shape of the stem is different for each different root. The growth scale value can control the range of the root tip; this does not affect the shape of the root, so we set all growth scale values to 1. Because all root models are seedlings, there is little difference in the length of the stem of all roots. Different roots also have different stem diameters, so we set the value of the stem diameters between 0.8 and 1.2. Cap Smoothing value can control the roundness of the root; we set its value between 0.2 and 0.5. crinkliness value can be used to control the degree of bending of the branches, and this value can control the complexity of the root; according to the common shape of a real apple seedling root, we set its value between 0.1 and 0.2. Seek Sun value is used to control how much the root bends upwards; if the value is very large, the root of the apple seedling will appear to upward growth, which is different from the real situation, so we set its value between 0.01 and 0.02.

Apple seedling roots have a lot of branches; we use random numbers to determine the shape and number of branches. The diameter of the branches is set between 0.3 and 0.7, and the number of branches is set between 10 and 30, which matches the real situation. The value of crinkliness is set to about 0.2, the growth direction of branches is usually more complex than that of the stem, so we set the Seek Sun value of branches to be between 0.2 and 0.3. By repeating this process, we finally designed a total of 800 different apple seedling roots 3D root models in our dataset; some examples are shown in Figure 1. Each 3D model has detailed parameters, the number, and thickness of each branch can be known, and every apple seedling root 3D model has been saved in obj format, which can be opened and observed in detail by common viewing software.

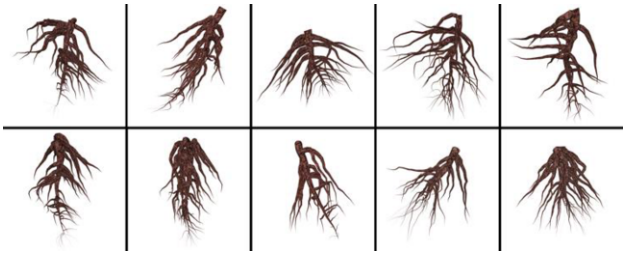

Figure 1. Apple Root 3D Models, each root is designed with the characteristics of a real apple root, with the main stem and several branches with different shapes.

3.2. Sweet Potato Root 3D Model Design

Sweet potato is a tangled herbaceous vine of the Dioscoreaceae family, and its root usually has multiple stems, which are elongated, and each stem has numerous whiskers. Through observation, we found that the number of stems of real sweet potato root is usually between 6 and 15, so in Unity3D, we set the number of stems for all 3D models between 6 and 15. In terms of diameter, the stem of the sweet potato root is much thinner than the apple's, so we set the diameter value of the stem to around 0.3. Because the shape of the sweet potato's stem is usually a straight line, so we set the value of Crinkliness to a small range, about 0.0002; this value is much smaller than the value of apple seedling roots. Sweet potato root does not have branches like apple seedling root, but all its items are distributed with numerous whiskers, and these whiskers are very thin and short; we set the radius value of all whiskers to 0.1 in Unity3D. As for the number of whiskers for each item, we set it to a value between 60 and 100, which is also the case for real sweet potatoes root. The growth direction and shape of these whiskers are very complex, so we set the value of whiskers to a larger range, around 0.03.

We repeated the process above 400 times, randomly setting different values each time. In the end, we got 400 different 3D models of sweet potato root; some examples are shown in Figure 2. Like the 3D models of apple seedling roots, each sweet potato roots 3D model has detailed parameters, and every 3D model has been saved in obj format.

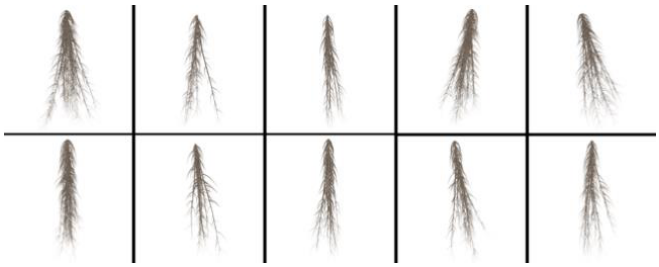

Figure 2. Sweet potato roots usually have multiple main stems, each of which is distributed with dense whiskers.

3.3 Extract Multi-angle 2D Images from 3D Models

After having 800 apple seedling roots and 400 sweet potato root 3D models, the next step we extract multi-angle 2D images from each 3D model. For a 3D model in a homogeneous coordinate system, we take the center point of the 3D model as the origin of the coordinate system. For a point coordinate (X, Y, Z) in the coordinate system, after rotating it around the Y-axis by an angle, a new position (X', Y', Z') is obtained, and the rotation matrix is shown in equation (1) and equation (2).

$$\begin{bmatrix} X' \\ Y' \\ Z' \end{bmatrix} = \begin{bmatrix} 1 & 0 & 0 \\ 0 & \cos\theta & \sin\theta \\ 0 & -\sin\theta & \cos\theta \end{bmatrix} \times \begin{bmatrix} X \\ Y \\ Z \end{bmatrix} \tag{1}$$

$$\begin{bmatrix} X'' \\ Y'' \\ Z'' \end{bmatrix} = \begin{bmatrix} \cos\theta & 0 & -\sin\theta \\ 0 & 1 & 0 \\ \sin\theta & 0 & \cos\theta \end{bmatrix} \times \begin{bmatrix} X \\ Y \\ Z \end{bmatrix} \quad (2)$$

In our work, we first take the center of the 3D model as the origin of the homogeneous coordinate system, rotated the 3D model counter clockwise around the Y-axis, and captured one 2D image every 10 degrees for a total of 360 degrees of rotation. Finally, we got 360 2D images of the 3D model rotated around the Y-axis. Then, we rotated the 3D model counter clockwise around the X-axis and took one 2D image every 10 degrees, and rotated 360 degrees; in the end, we got 36 2D images of the model rotated around the X-axis. The overall rotation process is shown in Figure 3.

Figure 3. Rotate along the Y-axis and X-axis, respectively, and take one 2D image every 10 degrees, and each model can get 72 images.

By repeating the above process, we first rotate all the root 3D models of apple seedlings to extract 2D images from different angles. We rotate all sweet potato root 3D models at different angles to extract 2D images. Finally, we extracted 72 2D images from different angles for each model. For 800 apple seedling roots and 400 sweet potato roots, we obtained a total of 86,400 2D images in our dataset, as shown in Figure 4.

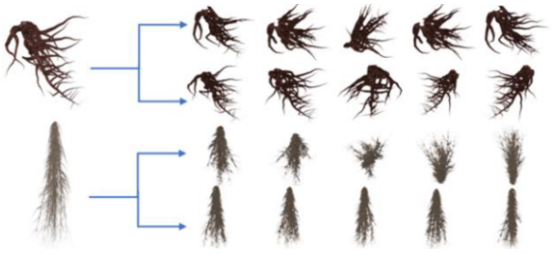

Figure 4. The left side is a 3D model, which is rotated to obtain a multi-angle 2D image. The upper right side is the images obtained along the X axis, and the bottom is the images obtained by rotating around the Y axis.

The above is the parameter setting process of the Sweet Potato Roots 3D Models in our dataset. We repeated this process 400 times, randomly setting different values each time. In the end, we got 400 different 3D models of sweet potato root; some examples are shown in Figure 4. Like the 3D models of apple seedling roots, each sweet potato roots 3D model has detailed parameters, and every 3D model has been saved in obj format.

Through the above work, our dataset has 800 3D models of apple seedling roots and 500 3D models of sweet potato roots, all of which are saved in obj format. Each 3D model corresponds to 72 images from different angles, and the resolution size of each image is 1080×1080, and it is saved in png format. All 3D models can be viewed in specific details, including the Diameter, length, and angle of items and branches. Some

other existing root datasets usually only provide 3D models without ground truth, while our dataset not only contains detailed parameters of 3D models but also provides corresponding multi-angle images. As far as we know, this is currently the only root dataset that provides these. Therefore, our data set can be easily used for the verification of various 3D reconstruction algorithms, which is of great help for the comparison of the effects of the algorithms. In the next section, we will test several 3D reconstruction algorithms with this dataset and give a comparison of the results.

4. Algorithm Testing

To test the usability of our dataset, we compare three different 3D reconstruction methods, namely Kinect Fusion, MVE (Multi-View Environment), and MVG+MVS. We use these methods to perform reconstruction tests on the roots in the dataset separately; some reconstruction results are shown in Figure 5. Thanks to the ground truth of the dataset, we can easily use the open-source software Cloud Compare to compare the reconstructed results with the original model in obj format; and to verify the accuracy of these methods. First, we matched the center of gravity between the original model and the reconstructed result; and then used the ICP algorithm in Cloud Compare to calculate the closest distance from any point in the reconstructed point cloud to the original model. In the experiment, we selected 40,000 patches for each analysis model. After the center ratio, we calculated the average distance and variance of each patch to the nearest point cloud of the original model in the 3D computing space. We used the average distance: M and variance: s as the indicators to evaluate the reconstruction accuracy, the calculation process is as shown in equation (3) and equation (4).

$$m = \frac{\sum_{i=1}^{n} |X_i - \hat{X}_i|}{n} \tag{3}$$

$$s = \sqrt{\frac{\sum_{i=1}^{n} (X_i - \hat{X}_i)^2}{n}} \tag{4}$$

In the above two equations, n is the number of paired points, $\hat{X}_i$ is the corresponding Euclidean distance after ICP registration, and $\hat{X}_i$ is the true value of the Euclidean distance of the corresponding point.

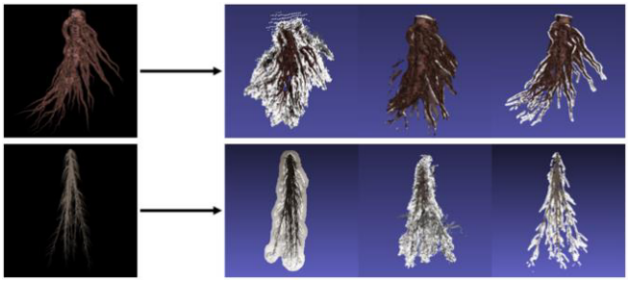

Figure 5. The left side is a 3D model, which is rotated to obtain a multi-angle 2D image. The upper right side is the images obtained by rotating along the X axis, and the bottom is the images obtained by rotating around the Y axis.

After getting the average distance m and variance of each reconstructed model, we sum them up, then calculate the mean distance: M and mean-variance: S of all models in the dataset; the statistical results are shown in Tables 1 and Table 2.

Table 1. 3D reconstruction accuracy statistics table of apple seedling roots.

Method	Kinect Fusion	MVE	MVG+MVS
M	1.42cm	0.831cm	0.475cm
S	0.1834	0.1645	0.1342

Table 2. 3D reconstruction accuracy statistics table of sweet potato roots.

Method	Kinect Fusion	MVE	MVG+MVS
M	1.03cm	0.619cm	0.212cm
S	0.1436	0.1542	0.1134

As seen from Table 1 and table 2, these three classic 3D reconstruction algorithms can be successfully tested on our dataset. Because our dataset has a good ground truth. Therefore, it can effectively reflect the performance of different 3D reconstruction algorithms. As seen from the table, among the reconstructions of these two different root models, Kinect Fusion has the worst performance, while MVG+MVS has relatively better results. But generally speaking, the reconstruction results of these algorithms are not ideal.

5. Conclusions

This paper introduces a new dataset that contains apple seedling root and sweet potato roots. This dataset contains 3D models and multi-angle pictures of apple and sweet potato roots. We use Unity 3D to make 3D models of the root, so each model has a good ground truth. The production process of the dataset is explained in detail, as well as the advantages of this dataset compared to existing datasets. However, the three-dimensional root model in this data set is still slightly different from the real root shape. Whether it can completely replace the real plant rhizome data set needs to be verified. This will be the next step of research. This datasets will be upload to the network and provided to every user who needs it for downloading and testing the 3D reconstruction algorithm.

Acknowledgments

This work was supported by the Jiangsu Agricultural Industry System [grant number JAST [2023] 345].

References

[1] Jia Z, Von Wirén N. Signaling pathways underlying nitrogen-dependent changes in root system architecture: from model to crop species. Journal of Experimental Botany, 2020, 71(15): 4393-4404.

[2] Wang J, Zhang Y, Gu R. Research status and prospects on plant canopy structure measurement using visual sensors based on three-dimensional reconstruction. Agriculture, 2020, 10(10): 462.

[3] Yandun F, Silwal A, Kantor G. Visual 3d reconstruction and dynamic simulation of fruit trees for robotic manipulation. Proceedings of the IEEE/CVF Conference on Computer Vision and Pattern Recognition Workshops. 2020: 54-55.

[4] Zhu R, Sun K, Yan Z, et al. Analysing the phenotype development of soybean plants using low-cost 3D reconstruction. Scientific Reports, 2020, 10(1): 1-17.
[5] Danilevicz M F, Bayer P E, Nestor B J, et al. Resources for image-based high-throughput phenotyping in crops and data sharing challenges. Plant physiology, 2021, 187(2): 699-715.
[6] Chiteri K O, Jubery T Z, Dutta S, et al. Dissecting the root phenotypic and genotypic variability of the Iowa mung bean diversity panel. Frontiers in Plant Science, 2022, 12: 808001.
[7] Samiei S, Rasti P, Ly Vu J, et al. Deep learning-based detection of seedling development. Plant Methods, 2020, 16: 1-11.
[8] Teng S, Hu X, Deng P, et al. Motion planning for autonomous driving: The state of the art and future perspectives. IEEE Transactions on Intelligent Vehicles, 2023.
[9] Mayer N, Ilg E, Hausser P, et al. A large dataset to train convolutional networks for disparity, optical flow, and scene flow estimation. Proceedings of the IEEE conference on computer vision and pattern recognition. 2016: 4040-4048.
[10] Gehrig M, Aarents W, Gehrig D, et al. Dsec: A stereo event camera dataset for driving scenarios. IEEE Robotics and Automation Letters, 2021, 6(3): 4947-4954.
[11] Li Y, Zhang T, Nakamura Y, et al. SplitFusion: Simultaneous tracking and mapping for non-rigid scenes. 2020 IEEE/RSJ International Conference on Intelligent Robots and Systems (IROS). IEEE, 2020: 5128-5134.
[12] Dai A, Nießner M, Zollhöfer M, et al. Bundlefusion: Real-time globally consistent 3D reconstruction using on-the-fly surface reintegration. ACM Transactions on Graphics (ToG), 2017, 36(4): 1.
[13] Schlarp J, Csencsics E, Schitter G. Design and evaluation of an integrated scanning laser triangulation sensor. Mechatronics, 2020, 72: 102453.
[14] Kim M, Kim J, Jung M, et al. Towards monocular vision-based autonomous flight through deep reinforcement learning. Expert Systems with Applications, 2022, 198: 116742.
[15] Wang Y, Cao R, Guan Y, et al. A Novel End-to-End Visual Odometry Framework Based on Deep Neural Network. 2022 International Conference on Computer Engineering and Artificial Intelligence (ICCEAI). IEEE, 2022: 528-532.
[16] Wang D, Cui X, Chen X, et al. Multi-view 3D reconstruction with transformers. Proceedings of the IEEE/CVF international conference on computer vision. 2021: 5722-5731.
[17] Fu K, Peng J, He Q, et al. Single image 3D object reconstruction based on deep learning: A review. Multimedia Tools and Applications, 2021, 80(1): 463-498.
[18] Mirzaei K, Arashpour M, Asadi E, et al. 3D point cloud data processing with machine learning for construction and infrastructure applications: A comprehensive review. Advanced engineering informatics, 2022, 51: 101501.